LSTM and Transformers based methods for Remaining Useful Life Prediction considering Censored Data

Jean-Pierre NOOT[1,2]
Etienne BIRMELE[1]
François REY[2]

[1] *Institut de Recherche Mathématique Avancée, UMR 7501 Université de Strasbourg et CNRS*
7 rue René-Descartes, 67000 Strasbourg, France
jnoot@unistra.fr
birmele@unistra.fr
[2] *Liebherr Components Colmar, Haut-Rhin, 68000, FRANCE*
jean-pierre.noot@liebherr.com
francois.rey@liebherr.com

ABSTRACT

Predictive maintenance deals with the timely replacement of industrial components relatively to their failure. It allows to prevent shutdowns as in reactive maintenance and reduces the costs compared to preventive maintenance. As a consequence, Remaining Useful Life (RUL) prediction of industrial components has become a key challenge for condition based monitoring. In many applications, in particular those for which preventive maintenance is the general rule, the prediction problem is made harder by the rarity of failing instances. Indeed, the interruption of data acquisition before the occurrence of the event of interest leads to right censored data. There are few articles in the literature that take that phenomenon into account for RUL prediction, even though it is common in the industrial environment to have a high rate of censored data.

The present article proposes a deep-learning approach based on multi-sensor time series which allows to consider censored data during the training of the neural networks. Two methods are proposed, respectively based on the Dual Aspect Self-Attention based on Transformer proposed by (Z. Zhang, Song, & Li, 2022) for non-censored data and on a recurrent neural network. Their evaluation on the C-MAPSS benchmark dataset shows, compared to the state-of-the-art RUL prediction methods, no loss in the absence of censoring, and outperformance on censored data.

1. INTRODUCTION

Technology and electronic developments of sensors nowadays allow the collection of huge amounts of data on mechanical and industrial equipment, in particular time series measuring their evolution over time. The definition of the maintenance schedule, which is crucial for the industry, therefore shifts to predictive, or condition-based maintenance (CBM). The latter is defined by opposition to the historical preventive maintenance, for which the maintenance schedule is pre-defined, each component being replaced at fixed time intervals. CBM avoids replacement of healthy components, and therefore reduces costs, by determining a dynamic schedule depending on the real-time monitoring of the system. A crucial step is therefore the estimation, given the actual status of the system, of the Remaining Useful Lifetime (RUL) of a component, that is the time before its failure.

Several approaches exist to create CBM models for RUL estimation (Arena, Collotta, Luca, Ruggieri, & Termine, 2021), most of them being model-based methods, data-driven methods or hybridisation of those approaches.

Model-based methods consider the physical phenomenon, for instance corrosion or fatigue, that leads to the failure. A mathematical model is used to simulate the studied mechanism and to get a RUL prediction (Tinga & Loendersloot, 2019). A precise physical and mechanical knowledge is however needed to build physical-based models. Moreover, this approach results in highly complex models when applied to large scale industrial systems composed with a lot of subsystems.

Data-driven methods regroup approaches that rely on stochas-

tic models or statistical analysis to create fault detection models not directly mimicking the underlying physics. It may consist in statistical algorithms to diagnose battery fault (Y. Zhao, Liu, Wang, & Hong, 2017), stochastic processes to mimic the degradation processes (Garay & Diedrich, 2019) or evolving fuzzy models for semiconductor health management (Boutrous, Bessa, Puig, Nejjari, & Palhares, 2022).

Data-driven methods include machine learning algorithms, which have been extensively used by the Prediction and Health Management community to establish predictive maintenance rules. Multiple linear regression durability models were for instance used to predict the fatigue life of automotive coil (Kong, Abdullah, Schramm, Omar, & Haris, 2019), or SVM classifiers for fault detection in vehicle suspensions (Jeong & Choi, 2019). In (Vasavi, Aswarth, Pavan, & Gokhale, 2021), a kNN classifier is used to detect fault by predicting vehicle health using real time data, while (Patil et al., 2018) relies on decision trees and gradient boosting regressor for RUL prediction.

Deep learning, like machine learning methods, allow to have no physical or mechanical knowledge of the studied system. In recent years, numerous articles have demonstrated the effectiveness of those methods for RUL prediction. The data at hand being mainly time series, the developed methods focus on architectures widely used to treat sequential data. Recurrent neural networks like Long-short-time-memory (LSTM) (Zheng, Ristovski, Farahat, & Gupta, 2017), or Convolutional neural network (CNN) (Sateesh Babu, Zhao, & Li, 2016) and recently Transformers (Z. Zhang et al., 2022), which were adapted from the original Transformer architecture (Vaswani et al., 2017) to deal with time series are popular method used to perform RUL predictions.

The presence of right-censored data is an important issue in many real-life industrial applications, which is not taken into account by most methods. Indeed, when the current policy on the field application is predictive maintenance, equipment's are renewed before failure, leading to numerous time-series in the dataset for which the RUL is unknown. One way to deal with such data is to use the survival approach based on Cox models that has been successfully transposed from medical analysis to maintenance analysis (Chen et al., 2020; Yang, Kanniainen, Krogerus, & Emmert-Streib, 2022). An alternative is the ordinal regression (OR) approach where the RUL prediction is replaced by a vector of predictions encoding the failure time (Vishnu, Malhotra, Vig, & Shroff, 2019).

The present paper deals with a new deep-learning method based on ordinal regression to predict RUL on censored data. It relies on two main contributions regarding the state of the art. Firstly, the DAST model (Z. Zhang et al., 2022) based on Transformers is adapted to an ordinal regression framework. Secondly, it is put onto competition with an improved of the LSTM-OR model (Vishnu et al., 2019) to obtain the final prediction rule.

To illustrate its performance, the proposed method is run on the C-MAPSS Turbofan NASA benchmark dataset, and compared to state-of-the-art methods, able to consider censored data or not. The benchmark dataset is being characterized by the absence of censor, the latter is artificially introduced at various levels. The proposed method is comparable to the best methods on non-censored data and better when a significant amount of data is censored.

2. Related Work

As stated in the introduction, the aim of this study is to consider the RUL prediction problem when the learning dataset is right-censored. That situation is common in applications, as such a censoring corresponds to components changed before the failure. This section introduces the main ideas of the DAST (Z. Zhang et al., 2022) and LSTM-OR (Vishnu et al., 2019) architectures, and then builds upon those ideas to propose a novel method for RUL estimation on censored data.

Beforehand, let us introduce the notations which will be used throughout the paper.

For a given unit, we denote by:

- $\mathrm{T}^\star$ the time of failure,
- C the censoring time if relevant, that is if the unit is replaced before failure,
- $\mathrm{T} = \min(\mathrm{C}, \mathrm{T}^\star)$ the observed time of replacement,
- X the time series of the p sensors data, $x_{k,t}$ being the measure of sensor k at time t,
- Z the optional of vector covariates, that is characteristics of the unit which are not varying with time.

Let us fix a maximum value R_{max} for the RUL estimation, which is standard procedure (Heimes, 2008; H. Li, Zhao, Zhang, & Zio, 2020) and is relevant for the applications, as it focuses on the precision of the method on the period preceding the failure. At a given time point t, we then define the lifetime to predict by

$$\mathrm{R}_t = \min(\mathrm{T}^\star - t, \mathrm{R}_{max})$$

Note that this lifetime is observed in the training set only when $\mathrm{T}^\star = \mathrm{T}$. If not, the only available information is that $\mathrm{R}_t \geq \min(\mathrm{C} - t, \mathrm{R}_{max})$.

All the variables in that section are in fact indexed by the number i of the considered unit, for instance when computing a loss. That index is omitted unless necessary for reading purposes.

2.1. Dual Aspect Self-Attention based on Transformer (DA-ST)

The DAST model is an encoder-decoder, with the specificity of a double encoding, using a time step encoder and the sensor encoder.

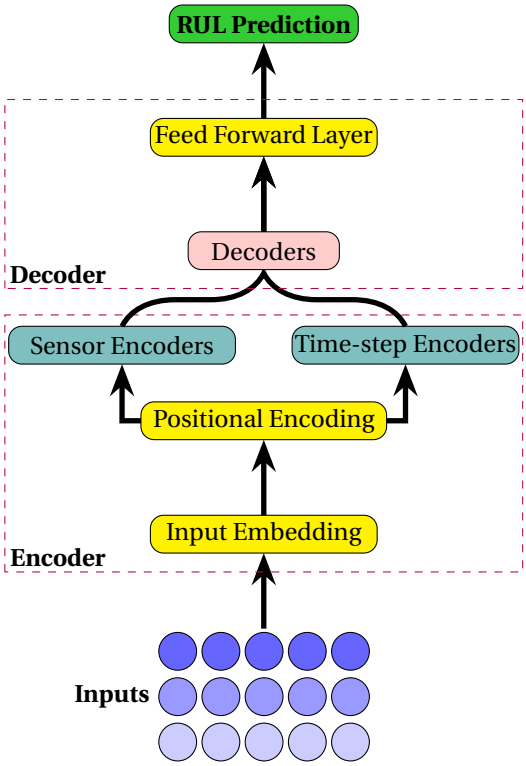

Figure 1. Original DAST architecture (Z. Zhang et al., 2022)

The input data of the DAST architecture consists in a decomposition of the times series X by a sliding window processing of width W, as shown in Figure 2. The input is thus a list of matrices (X_t), each of size (p, W):

$$X_t = \begin{pmatrix} x_{1,t} & \cdots & x_{1,t+W} \\ \vdots & \ldots & \vdots \\ x_{p,t} & \cdots & x_{p,t+W} \end{pmatrix} \quad (1)$$

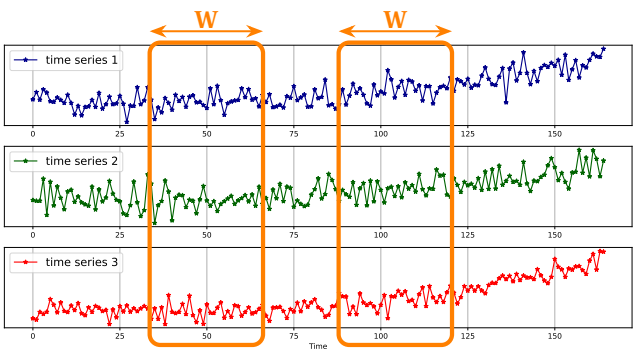

Figure 2. Example of sliding window of size W for time-series on 3 sensors

The data of each window are normalized to equalize the amplitude for each sensor and completed with positional encoding to keep track of the relative time positions of the columns as well as constant lines corresponding to the covariates Z. It is also enriched for each sensor by the mean value and the slope of the linear regression as a function of time, as proposed in (Song et al., 2020).

The originality of DAST is to consider these inputs in two dimensions. On the one hand, the enriched matrix X_t is given as input of the time step encoder, which encodes through self-attention scores per time point the dependency between the vectors of data at different time points. On the other hand, its transpose X_t^T is given as input to the sensor encoder which uses the same architecture to encode and capture the dependency information between the sensors. A final fusion layer finally allows to mix both encodings into a final one, which contains the importance of different combinations of sensors and time steps at the same time. That information is valuable in the context of RUL estimation and is processed by the decoder part of the architecture to obtain a prediction.

As the prediction is a scalar corresponding to $\hat{R}_t$, the model is trained using a RMSE loss, that is the square root of the mean squared prediction error when summing over all units i and time points t.

2.2. Ordinal Regression for RUL Estimation with censored data

In various applications, the complete lifetime of the units is not systematically available as the components may be changed before failure, leading to right-censored lifetime. Direct RUL estimation requires the complete lifetime of the components in the learning data set and thus discards such data, which may represent most of the available data. One possible method to integrate both right-censored and uncensored lifetime data, is the ordinal regression approach developed in (Vishnu et al., 2019).

The key idea is to discretize the object to be estimated, by replacing the RUL $R_t^\star$ by a binary vector of the component status in the future. To do so, two integers L and K are fixed and the status of the unit is checked one time every L cycles (or time points in the time series). The new target is then a vector Y_t of length K where

$$y_{t,k} = \begin{cases} 0 & \text{if} \quad T > t + kL, \\ & \text{i.e. the unit is healthy after } k * L \text{ cycles}, \\ 1 & \text{if} \quad T \leq t + kL \quad \text{and} \quad T = T^\star, \\ & \text{i.e. the unit has failed before } k * L \text{ cycles}, \\ - & \text{if} \quad T \leq t + kL \quad \text{and} \quad T = C, \\ & \text{i.e. the unit status is unknown after } k * L \text{ cycles} \end{cases}$$

t is the time of the current time step and k is the index of Y_t.

Let us for example consider L = 10 and K = 10:

- if the component fails after 75 cycles, $Y_t = (0,0,0,0,0,0,0,0,1,1,1)$,
- if the component is replaced after 75 cycles but before failure $Y_t = (0,0,0,0,0,0,0,0,-,-,-)$. The last three elements are masked as no status appropriate for learning is available.

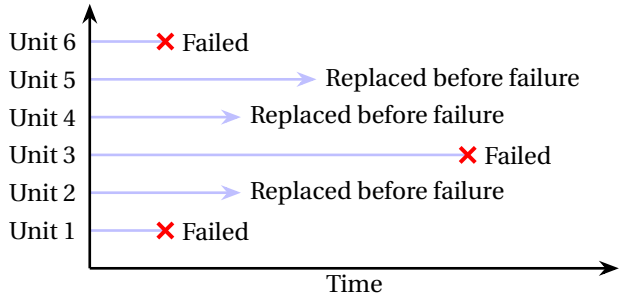

Figure 3. Right-censored data: unit 2, 4 and 5 are censored to the right, they were still healthy when replaced

A learning phase applied on the binary vectors of the training set allows then to obtain a prediction rule, as initially proposed using an LSTM architecture (Vishnu et al., 2019). The prediction for a given unit at time t, denoted by $\hat{Y}_t$, is a vector of K probabilities indicating the probability of failure before the corresponding time steps.

As the problem has become a binary classification problem, the learning is done using the binary cross-entropy (BCELoss). It is however adjusted for right-censored data by discarding all coordinates equal to - in the Y vectors. For example, if $Y_t = (0,0,0,0,0,0,0,0,-,-,-)$, its contribution to the loss is only computed on the seven first coordinates. In other terms, the loss is the sum over all units i and times t of

$$\mathrm{BCE}(Y_t, \hat{Y}_t) = -\sum_{k=1}^{K} \left(y_{t,k} log(\hat{y}_{t,k}) + (1 - y_{t,k}) log(1 - \hat{y}_{t,k}) \right) \tag{2}$$

where the term in the sum is set to 0 whenever $y_{t,k}$ is masked.

2.3. The proposed method

We consider a framework to deal with censored data using the OR encoding with the following step:

1. Adapt the DAST architecture to the OR framework by adding a sigmoid layer, leading to the **DAST-OR** architecture. After training, it outputs a vector $(\hat{Y}_t)$ of length K for every time point in a time series.
2. Following (Chaoub, Voisin, Cerisara, & Iung, 2021) which studies LSTM for RUL prediction, a feed-forward-layer is added in the LSTM-OR architecture, between the LSTM and the sigmoid output layer.This model is denoted as **LSTM-MLP-OR**. It outputs an alternative vector $(\hat{Y}_t)$ of length K for every time point in a time series.
3. Map every vector $\hat{Y}_t$ into a predicted RUL $\hat{R}_t$, following (Vishnu et al., 2019):

$$\hat{R}_t = R_{max}(1 - \frac{1}{K}\sum_{k=1}^{K} \hat{y}_{t,k}) \tag{3}$$

with $R_{max} = KL$ being chosen as the length of the time interval covered by $\hat{Y}_t$.

4. Select the best model in terms of RMSE loss of this RUL prediction on the validation data.

Note that the RUL estimation introduced step 3 is of practical use, but also allows comparison with methods in the literature estimating directly the RUL.

Moreover, to reduce randomness, 10 train of each model are performed, leading to two options:

1. **The simple model:** The model with the best loss on the validation dataset is chosen.
2. **The ensemble model:** We consider an ensemble of models, the final prediction corresponding to the average prediction of the 6 best models among the 10 models trained.

3. Experimental Evaluation

3.1. The CMAPSS dataset

The performance of the proposed method is evaluated on the **C-MAPSS** (Commercial Modular Aero Propulsion System Simulation) dataset, which is used as a benchmark for RUL estimation methods. It simulates run-to-failure trajectories of turbofan engines (Saxena, Goebel, Simon, & Eklund, 2008) in two different operating conditions and two failure modes, leading to four sub-datasets FD001, FD002, FD003 and FD004. The characteristics of the four sets are summarized in Table 1. Each trajectory contains the following variables:

1. a unit number corresponding to the component identifier,
2. a time variable corresponding to the number of cycles performed,
3. the simulation parameters (operating condition and failure modes),
4. the simulated data from 21 sensors.

Table 1. Summary of C-MAPSS dataset

C-MAPSS sub-datasets	FD001	FD002	FD003	FD004
Train trajectories	100	260	100	249
Test trajectories	100	259	100	248
Operating condition	1	6	1	6
Fault modes	1	1	2	2

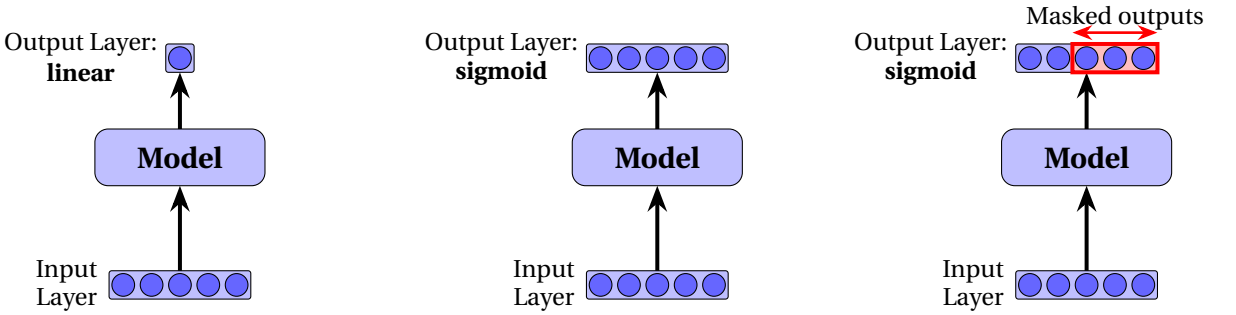

(a) Metric regression (b) Ordinal regression (c) Ordinal regression with censored data

Figure 4. Metric regression compared to ordinal regression

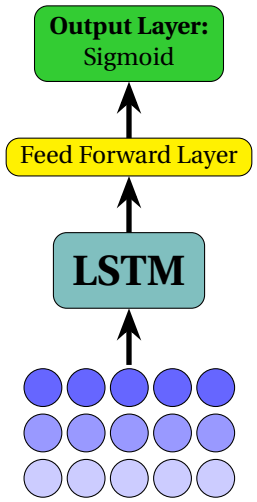

Figure 5. LSTM-MLP-OR architecture

3.2. Data preprocessing and censoring

Sensors having a constant value during the experiment are removed, leaving 14 sensors for datasets FD001 and FD003, and 21 for datasets FD002 and FD004. Data standardization is processed on the remaining sensors by removing the mean and scaling by standard deviation.

Right-censoring is artificially added to the data, with rates $p_c \in [0\%, 20\%, 50\%, 70\%, 90\%]$. More precisely, for every censor rate p_c, the corresponding fraction of the units are randomly chosen, and, for each selected unit, the time series are truncated prior to failure at a random moment. When $p_c = 90\%$, it leads to a train set where only 10% of the units have a known RUL, and approximately 45% of the initial data is kept.

Finally, to be able to chose the best models during the training, each sub-dataset is divided into a training set and a validation set, 20% of randomly chosen units joining the validation set.

3.3. Trained models

Three architectures are trained on the four datasets of the CMAPSS data:

1. **DAST for RUL** (Z. Zhang et al., 2022),
2. **LSTM-MLP-OR**,
3. **DAST-OR**.

Moreover, each of them are trained ten times, and those results are used to derive a single and an ensemble model for each architecture. Ensemble models are denoted with the addition of a final E, for instance DAST-ORE for the ensemble version of DAST-OR.

We also consider the model **BEST-ORE** which is chosen between DAST-ORE and LSTM-MLP-ORE based on the RMSE on the validation dataset.

Seven different models are thus obtained, which can be fairly compared, on exactly the same preprocessing, censoring, as well as training, validation and test sets.

For all models, we use $R_{max} = 130$, and for the methods relying on ordinal regression, we consider Y vectors consisting on K = 13 coordinates corresponding to the status every L = 10 cycles.

3.4. Hyperparameters of the models

The hyperparameters employed for the DAST are those described in the original article (Z. Zhang et al., 2022), except for number of epochs that is set to 250 with early stopping. They are summarized table 2.

The hyperparameters for DAST-OR are essentially identical. Table 3 presents those which are specific to DAST-OR (sigmoid output layer and loss) or are chosen different (a manual tuning on the window size gave better results). The number of epochs is set to 500 with early stopping.

The hyperparameters of the LSTM-MLP-OR model mainly correspond to the article introducing LSTM-OR (Vishnu et al., 2019). However, not all parameters being explicitly de-

Table 2. Hyperparameters of DAST

Hyperparameter	Value
Input embedding	1 MLP layer with 64 neurons, activation: Linear
Sensor encoder	N = 2 Sensor encoder blocks with H = 4 heads
Time step encoder	N = 2 Timestep encoder blocks with H = 4 heads
Decoder	N = 1 Decoder block with H = 4 heads
Output layer	1 MLP layer with 64 neurons, activation: ReLU
Final output layer	1 MLP layer with 1 neurons, activation: Linear
Learning Rate	0.001
Batch Size	256
Dropout	0.2
Window Size	40 for FD001 and FD003, 60 for FD002 and FD004
Optimizer	Rectified Adam
Loss	RMSE

Table 3. Hyperparameters of DAST-OR

Hyperparameter	Value
Final output layer	1 MLP layer with 13 neurons, activation: Sigmoid
Window Size	60 for FD001 and FD003, 80 for FD002 and FD004
Loss	BCELoss

tailed in the original article, manual tuning has been applied to the LSTM-MLP-OR model with a few trials on the validation set.

3.5. Results on uncensored data

This part focuses on the comparison of the results obtained on data without censoring. Table 4 shows the results for the seven trained models on each of the four datasets, with various state-of-the-art methods. Note that the seven methods are trained with the same preprocessing and separation into training and validation sets, whereas the reported values for other methods correspond those indicated in the corresponding publications. Small variations may therefore not be significant.

On FD001, results of DAST-ORE are equivalent to the results of DAST and F+T. On FD002 results of LSTM-MLP-OR and LSTM-MLP-ORE are significantly better than the results obtain with DAST, and equivalent to results obtain with MLP+LSTM and F+T. On FD003 DAST-ORE perform better than other models of the state of the art. The results of LSTM-MLP-ORE are equivalent to the result of MLP+LSTM and F+T. On FD004 LSTM-MLP-ORE perform significantly better than other models. All the OR method proposed are significantly better than the LSTM-ORCE.

Two main conclusions can be drawn from those results. The first is that, even if OR models were designed to handle right-censored data, the obtained results on uncensored data are equivalent to those found in the literature with models specifically made for direct RUL estimation. The second interesting fact to note is the dependence on the number of operating conditions in the dataset (cf Table 1). Differences between sets FD001 and FD003, with a unique operating condition, and sets FD002 and FD004, with six different ones, are commonly found in the state of the art (C. Zhao, Huang, Li, & Yousaf Iqbal, 2020) (Sateesh Babu et al., 2016) (C. Zhang, Lim, Qin, & Tan, 2016) (Zheng et al., 2017) (X. Li, Ding, & Sun, 2018). Furthermore, the number of inputs used between is different. In this study, it appears that DAST-based methods are more powerful when the operating condition is unique, while LSTM-based outperform them when there are 6 operating conditions. Learning both architectures and keeping the best on the validation set, as does BEST-ORE, is therefore useful.

3.6. Results on censored data

The results on the C-MAPSS dataset for each right-censored rate are detailed in Tables 6 and 5. The former compares the proposed ensemble methods to the ensemble LSTM-ORCE method (Vishnu et al., 2019) for the data subsets (FD001 and FD004) and censoring rates studied in that article. The train and validation sets being different, small variations should not be interpreted. However, it clearly indicates a better performance of DAST-ORE on FD001 and a significant improvement with LSTM-MLP-ORE due to the supplementary MLP layer on FD004.

Table 6 shows the results for the models listed in section 3.3 trained on the same training and validation data. For readability, BEST-ORE is not indicated, but the associated RMSE is always the lowest among the RMSEs of LSTM-MLP-ORE and DAST-ORE.

The FD001 dataset has more simple operating conditions and more simple failure modes than the other C-MAPSS sub-datasets. On FD001 the DAST-ORE model has the best RMSE for each percentage of right-censored value. With the increase of p_c, the RMSE is slowly deteriorating and reach it's worst value at $p_c = 90\%$, which is not a surprise as the learning data becomes less informative. Other models, especially LSTM-based ones, show a bigger deterioration with increasing censoring.

The results are similar on FD003, which has also only one operating condition but two failure modes. The best overall results are obtained with DAST-ORE. Moreover, the increasing of the RMSE for highly censored data is milder for DAST-ORE than for competing methods.

FD002 and FD004 are considered more complex than FD001

Table 4. RMSE results on the C-MAPSS dataset without censoring

Model	**FD001**	**FD002**	**FD003**	**FD004**	Average RMSE
LSTM-MLP-OR	14.24	**12.00**	17.27	15.35	14.94
LSTM-MLP-ORE	13.20	12.77	13.84	14.75	13.64
DAST	12.35	16.48	13.43	19.89	15.54
DAST-E	12.22	15.44	12.89	16.14	14.17
DAST-OR	12.16	15.62	9.64	16.20	13.41
DAST-ORE	11.57	15.55	**8.54**	18.01	13.42
BEST-ORE	11.57	12.77	**8.54**	14.75	**11.91**
DAST (Z. Zhang et al., 2022)	**11.43**	15.25	11.32	18.36	14.09
LSTM-ORCE (Vishnu et al., 2019)	14.62	-	-	27.47	-
MLP+LSTM (Chaoub et al., 2021)	13.26	12.49	13.11	**13.97**	13.21
F+T (Lai, Liu, Pan, & Chen, 2022)	**11.43**	13.32	11.47	14.38	12.65

Table 5. Results RMSE on C-MAPSS

	FD001					
p_c	LSTM-MLP-OR	LSTM-MLP-ORE	DAST	DAST-E	DAST-OR	DAST-ORE
0%	14.24	13.20	12.35	12.22	12.16	**11.57**
20%	15.42	14.01	13.69	12.59	12.73	**12.51**
50%	15.09	15.96	15.41	13.37	13.39	**12.99**
70%	17.83	17.97	15.38	14.08	14.28	**12.51**
90%	30.02	26.76	16.78	17.17	17.01	**15.80**
	FD002					
p_c	LSTM-MLP-OR	LSTM-MLP-ORE	DAST	DAST-E	DAST-OR	DAST-ORE
0%	**12.00**	12.77	16.48	15.44	15.62	15.55
20%	15.43	**13.01**	14.09	13.80	16.37	18.51
50%	13.71	**13.15**	15.08	14.18	15.39	16.58
70%	14.24	**13.24**	16.10	14.74	16.71	17.73
90%	16.44	**13.61**	15.85	15.08	25.23	17.00
	FD003					
p_c	LSTM-MLP-OR	LSTM-MLP-ORE	DAST	DAST-E	DAST-OR	DAST-ORE
0%	17.27	13.84	13.43	12.89	9.64	**8.54**
20%	15.69	12.80	13.55	12.53	10.03	**8.81**
50%	13.97	13.46	16.04	12.57	11.69	**10.14**
70%	21.72	21.13	20.88	15.32	13.46	**12.20**
90%	38.74	30.66	22.34	22.88	19.59	**16.09**
	FD004					
p_c	LSTM-MLP-OR	LSTM-MLP-ORE	DAST	DAST-E	DAST-OR	DAST-ORE
0%	16.23	**14.75**	19.89	16.14	16.20	18.01
20%	15.66	**14.42**	18.32	15.23	18.01	16.93
50%	16.00	**14.67**	17.46	15.66	17.43	19.49
70%	16.59	**15.11**	17.32	17.10	14.84	20.83
90%	18.85	**15.47**	19.79	17.21	22.41	22.14

Table 6. RMSE results on FD001-FD004 with censor

p_c	LSTM-MLP-ORE	DAST-ORE	LSTM-ORCE (Vishnu et al., 2019)
	FD001		
50%	15.96	**12.99**	15.98
70%	17.97	**12.51**	16.57
90%	26.76	**15.80**	20.38
	FD004		
50%	**14.67**	19.49	30.62
70%	**15.11**	20.83	31.27
90%	**15.47**	22.14	38.41

and FD003, because they mix several operating conditions. In both cases, the LSTM-based models outperform the DAST-based ones, as for uncensored data, with a small advantage for the LSTM-MLP-ORE ensemble method. In those two cases, the decrease of performance with growing censoring is remarkably low.

The conclusion of this study is therefore two-fold. First, the competition between LSTM and DAST-based architectures remains relevant with censored data, as different conditions may lead to different rankings of those methods. Second, OR-based methods allow to obtain a reasonable loss of performance when the real time of failure is missing for most of the learning data.

As prescribed in (Saxena et al., 2008), the results were evalu-

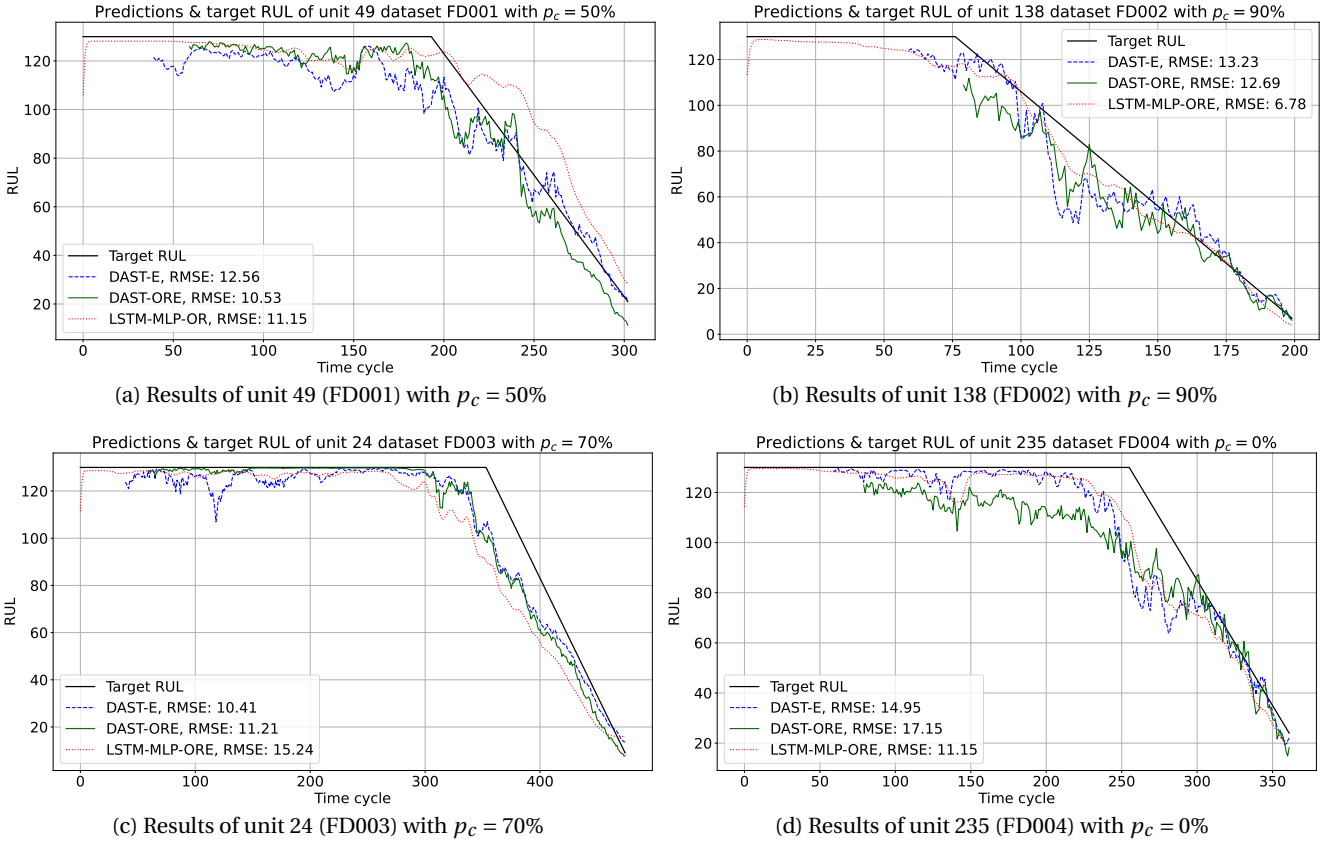

(a) Results of unit 49 (FD001) with $p_c = 50\%$

(b) Results of unit 138 (FD002) with $p_c = 90\%$

(c) Results of unit 24 (FD003) with $p_c = 70\%$

(d) Results of unit 235 (FD004) with $p_c = 0\%$

Figure 6. Example of results on one units of each sub-dataset

ated by the RMSE on the predictions of the last time-point of the time-series in the test set. To illustrate more visually the results of the different methods, Figure 6 provides some plots of the predictions of the ensemble methods for randomly picked time series on different datasets and censoring rates.

3.7. Asymmetric score evaluation

Prediction on C-MAPSS should also be evaluated by the asymetric score (Saxena et al., 2008) defined by

$$\text{Score} = \begin{cases} e^{\frac{\hat{\text{R}}_t - \text{R}_t}{13}} - 1 & \text{if } \hat{\text{R}}_t - \text{R}_t \geq 0 \\ e^{-\frac{\hat{\text{R}}_t - \text{R}_t}{13}} - 1 & \text{if } \hat{\text{R}}_t - \text{R}_t < 0 \end{cases}$$

That score corresponds to a higher penalty for overestimation rather underestimation of the RUL.

Table 7 shows the scores for the ensemble methods DAST-E, DAST-ORE and LSTM-ORE. If the results are rather coherent with the RMSE comparisons for FD001 and FD003, the advantage of LSTM-based methods compared to DAST-E is less clear for FD002 and FD004.

However, it has to be noted that the OR-based methods were trained with a symmetric BCELoss which does not take into consideration a different penalty for over and under-estimations. In terms of binary vectors, it means a higher penalty for a close to 0 coordinate in $\hat{\text{Y}}_t$ when the truth is 1 (the fan is predicted running when it actually failed, which is an over-estimation of the RUL) than for a prediction close to 1 when the truth is 0.

A possibility to introduce this asymmetry would be to consider a modified loss by replacing Equation 2 by

$$\text{BCE}(\text{Y}_t, \hat{\text{Y}}_t) = -\sum_{k=1}^{\text{K}} \left(\alpha y_{t,k} log(\hat{y}_{t,k}) + (1 - y_{t,k}) log(1 - \hat{y}_{t,k})\right) \tag{4}$$

where $\alpha > 1$ is a hyperparameter to be optimized.

4. Conclusion

This work addresses the challenge of estimating the Remaining Useful Life (RUL) of industrial components from time series data with no prior physical model of the system and a high rate of censored data. It does so by considering two data-driven deep-learning architectures relying on the ordi-

Table 7. Score results on C-MAPSS

	FD001		
p_c	LSTM-MLP-ORE	DAST-E	DAST-ORE
0%	341.00	**201.17**	206.48
20%	410,63	**232,49**	269,68
50%	631,91	**252,89**	296,04
70%	1279,51	458,45	**261,79**
90%	4566,18	808,5	**500,21**
	FD002		
p_c	LSTM-MLP-ORE	DAST-E	DAST-ORE
0%	708,28	**638,34**	978,48
20%	753,57	**531,06**	1891,21
50%	751,84	**544,1**	1412,07
70%	786,58	**647,39**	1362,25
90%	860,19	**849,25**	1286,1
	FD003		
p_c	LSTM-MLP-ORE	DAST-E	DAST-ORE
0%	322,06	206,94	**103,65**
20%	250,9	192,28	**111,17**
50%	267,75	223,95	**143,29**
70%	1611,57	437,85	**272,35**
90%	3100,45	2797,84	**447,64**
	FD004		
p_c	LSTM-MLP-ORE	DAST-E	DAST-ORE
0%	**1741,67**	2262,98	2739,62
20%	1772,3	**1518,44**	2591,59
50%	**1434,33**	2206,4	2788,02
70%	**2096,04**	2470,12	3863,9
90%	1689,67	**1194,16**	2903,72

nal regression approach introduced in (Vishnu et al., 2019) for RUL estimation. One of them is an improved version of the LSTM-OR method by (Vishnu et al., 2019), the second is an adaptation to censored data of the DAST model introduced in (Z. Zhang et al., 2022).

These approaches are shown to perform as well on the C-MAPSS data as the existing direct RUL estimation methods found in the literature on uncensored data, and better on censored data.

Furthermore, the two proposed architectures are shown to be complementary, as they outperform each other depending on the complexity of the dataset. Therefore, in the context of estimating the lifespan of components, it is interesting to put them in competition, considering that this approach should yield favorable results regardless of the complexity of the data and the rate of right-censored data.

CODE AVAILABILITY

The code was written in Pytorch and is available at https://gitlab.math.unistra.fr/jnoot/rul_estimation_cmapss

REFERENCES

Arena, F., Collotta, M., Luca, L., Ruggieri, M., & Termine, F. G. (2021). Predictive maintenance in the automotive sector: A literature review. *Mathematical and Computational Applications*, *27*(1), 2.

Boutrous, K., Bessa, I., Puig, V., Nejjari, F., & Palhares, R. M. (2022). Data-driven prognostics based on evolving fuzzy degradation models for power semiconductor devices. In *Phm society european conference* (Vol. 7, pp. 68–77).

Chaoub, A., Voisin, A., Cerisara, C., & Iung, B. (2021). Learning representations with end-to-end models for improved remaining useful life prognostics. *arXiv preprint arXiv:2104.05049*.

Chen, C., Liu, Y., Wang, S., Sun, X., Di Cairano-Gilfedder, C., Titmus, S., & Syntetos, A. A. (2020). Predictive maintenance using cox proportional hazard deep learning. *Advanced Engineering Informatics*, *44*, 101054.

Garay, J. M., & Diedrich, C. (2019). Analysis of the applicability of fault detection and failure prediction based on unsupervised learning and monte carlo simulations for real devices in the industrial automobile production. In *2019 ieee 17th international conference on industrial informatics (indin)* (Vol. 1, pp. 1279–1284).

Heimes, F. O. (2008). Recurrent neural networks for remaining useful life estimation. In *2008 international conference on prognostics and health management* (pp. 1–6).

Jeong, K., & Choi, S. (2019). Model-based sensor fault diagnosis of vehicle suspensions with a support vector machine. *International Journal of Automotive Technology*, *20*, 961–970.

Kong, Y., Abdullah, S., Schramm, D., Omar, M., & Haris, S. (2019). Development of multiple linear regression-based models for fatigue life evaluation of automotive coil springs. *Mechanical Systems and Signal Processing*, *118*, 675–695.

Lai, Z., Liu, M., Pan, Y., & Chen, D. (2022). Multi-dimensional self attention based approach for remaining useful life estimation. *arXiv preprint arXiv:2212.05772*.

Li, H., Zhao, W., Zhang, Y., & Zio, E. (2020). Remaining useful life prediction using multi-scale deep convolutional neural network. *Applied Soft Computing*, *89*, 106113.

Li, X., Ding, Q., & Sun, J.-Q. (2018). Remaining useful life estimation in prognostics using deep convolution neural networks. *Reliability Engineering & System Safety*, *172*, 1–11.

Patil, S., Patil, A., Handikherkar, V., Desai, S., Phalle, V. M., & Kazi, F. S. (2018). Remaining useful life (rul) prediction of rolling element bearing using random forest and gradient boosting technique. In *Asme international mechanical engineering congress and exposition* (Vol. 52187, p. V013T05A019).

Sateesh Babu, G., Zhao, P., & Li, X.-L. (2016). Deep convolutional neural network based regression approach for estimation of remaining useful life. In *Database systems for advanced applications: 21st international conference, dasfaa 2016, dallas, tx, usa, april 16-19, 2016, proceedings, part i 21* (pp. 214–228).

Saxena, A., Goebel, K., Simon, D., & Eklund, N. (2008). Damage propagation modeling for aircraft engine run-to-failure simulation. In *2008 international conference on prognostics and health management* (pp. 1–9).

Song, Y., Gao, S., Li, Y., Jia, L., Li, Q., & Pang, F. (2020). Distributed attention-based temporal convolutional network for remaining useful life prediction. *IEEE Internet of Things Journal*, *8*(12), 9594–9602.

Tinga, T., & Loendersloot, R. (2019). Physical model-based prognostics and health monitoring to enable predictive maintenance. *Predictive Maintenance in Dynamic Systems: Advanced Methods, Decision Support Tools and Real-World Applications*, 313–353.

Vasavi, S., Aswarth, K., Pavan, T. S. D., & Gokhale, A. A. (2021). Predictive analytics as a service for vehicle health monitoring using edge computing and ak-nn algorithm. *Materials Today: Proceedings*, *46*, 8645–8654.

Vaswani, A., Shazeer, N., Parmar, N., Uszkoreit, J., Jones, L., Gomez, A. N., ... Polosukhin, I. (2017). Attention is all you need. *Advances in neural information processing systems*, *30*.

Vishnu, T., Malhotra, P., Vig, L., & Shroff, G. (2019). Data-driven prognostics with predictive uncertainty estimation using ensemble of deep ordinal regression models. *International Journal of Prognostics and Health Management*, *10*(4).

Yang, Z., Kanniainen, J., Krogerus, T., & Emmert-Streib, F. (2022). Prognostic modeling of predictive maintenance with survival analysis for mobile work equipment. *Scientific Reports*, *12*(1), 8529. Retrieved from https://doi.org/10.1038/s41598-022-12572-z doi: 10.1038/s41598-022-12572-z

Zhang, C., Lim, P., Qin, A. K., & Tan, K. C. (2016). Multiobjective deep belief networks ensemble for remaining useful life estimation in prognostics. *IEEE transactions on neural networks and learning systems*, *28*(10), 2306–2318.

Zhang, Z., Song, W., & Li, Q. (2022). Dual aspect self-attention based on transformer for remaining useful life prediction. *IEEE Transactions on Instrumentation and Measurement*, *71*, 1–11.

Zhao, C., Huang, X., Li, Y., & Yousaf Iqbal, M. (2020). A double-channel hybrid deep neural network based on cnn and bilstm for remaining useful life prediction. *Sensors*, *20*(24), 7109.

Zhao, Y., Liu, P., Wang, Z., & Hong, J. (2017). Electric vehicle battery fault diagnosis based on statistical method. *Energy Procedia*, *105*, 2366–2371.

Zheng, S., Ristovski, K., Farahat, A., & Gupta, C. (2017). Long short-term memory network for remaining useful life estimation. In *2017 ieee international conference on prognostics and health management (icphm)* (pp. 88–95).